Nonfactorizable contributions to $B \to D^{(*)}M$ decays

Yong-Yeon Keum,[1,*] T. Kurimoto,[2,†] Hsiang-nan Li,[3,‡] Cai-Dian Lü,[4,§] and A. I. Sanda[1,‖]

[1]*Department of Physics, Nagoya University, Nagoya, Japan*
[2]*Faculty of Science, Toyama University, Toyama 930-8555, Japan*
[3]*Institute of Physics, Academia Sinica, Taipei, Taiwan 115, Republic of China*
and Department of Physics, National Cheng-Kung University, Tainan, Taiwan 701, Republic of China
[4]*CCAST (World Laboratory), P. O. Box 8730, Beijing 100080, China*
and Institute of High Energy Physics, CAS, P. O. Box 918(4), Beijing 100039, China[¶]

While the naive factorization assumption works well for many two-body nonleptonic B meson decay modes, the recent measurement of $\bar{B} \to D^{(*)0}M^0$ with $M = \pi$, ρ, and ω shows a large deviation from this assumption. We analyze the $B \to D^{(*)}M$ decays in the perturbative QCD approach based on the k_T factorization theorem, in which both factorizable and nonfactorizable contributions can be calculated in the same framework. Our predictions for the Bauer-Stech-Wirbel parameters, $|a_2/a_1| = 0.43 \pm 0.04$ and $\mathrm{Arg}(a_2/a_1) \sim -42°$ and $|a_2/a_1| = 0.47 \pm 0.05$ and $\mathrm{Arg}(a_2/a_1) \sim -41°$, are consistent with the observed $B \to D\pi$ and $B \to D^*\pi$ branching ratios, respectively. It is found that the large magnitude $|a_2|$ and the large relative phase between a_2 and a_1 come from color-suppressed nonfactorizable amplitudes. Our predictions for the $\bar{B}^0 \to D^{*0}\rho^0, D^{*0}\omega$ branching ratios can be confronted with future experimental data.

PACS number(s): 13.25.Hw, 11.10.Hi, 12.38.Bx, 13.25.Ft

I. INTRODUCTION

Understanding nonleptonic B meson decays is crucial for testing the standard model, and also for uncovering a trace of new physics. The simplest case is two-body nonleptonic B meson decays, for which Bauer, Stech, and Wirbel (BSW) proposed the naive factorization assumption (FA) in their pioneering work [1]. Considerable progress, including the generalized FA [2–4] and QCD-improved FA (QCDF) [5], has been made since this proposal. On the other hand, a technique to analyze hard exclusive hadronic scattering was developed by Lepage and Brodsky [6] based on the collinear factorization theorem in perturbative QCD (PQCD). A modified framework based on the k_T factorization theorem was then given in [7,8], and extended to exclusive B meson decays in [9–12]. The infrared finiteness and gauge invariance of the k_T factorization theorem was shown explicitly in [13]. Using this so-called PQCD approach, we investigate the dynamics of nonleptonic B meson decays [14–16]. Our observations are summarized as follows.

(1) The FA holds approximately for charmless B meson decays, as our computation shows that nonfactorizable contributions are always negligible due to the cancellation between a pair of nonfactorizable diagrams.

(2) Penguin amplitudes are enhanced, as the PQCD formalism includes dynamics from the region where the energy scale μ runs to $\sqrt{\bar{\Lambda} m_b} < m_b$, $\bar{\Lambda} \equiv m_B - m_b$ being the B meson and b quark mass difference.

(3) Annihilation diagrams contribute to large short-distance strong phases through the $(S+P)(S-P)$ penguin operators.

(4) The sign and the magnitude of CP asymmetries in two-body nonleptonic B meson decays can be calculated, and we have predicted relatively large CP asymmetries in the $B \to K^{(*)}\pi$ [14,17] and $\pi\pi$ modes [15,16,18].

All analyses involving strong dynamics suffer larger theoretical uncertainties than we would like. How reliable are these predictions? This can be answered only by comparing more of our predictions with experimental data. For this purpose, we study the $B \to D^{(*)}M$ decays in PQCD, where M is a pseudoscalar or a vector meson. A $D^{(*)}$ meson is massive, and the energy release involved in two-body charmed decays is not very large. If predictions for these decays agree reasonably well with experimental data, PQCD should be more convincing for two-body charmless decays. Since penguin diagrams do not contribute, there are fewer theoretical ambiguities, such as the arguments about chiral or dynamical enhancement. Checking the validity of PQCD analyses in charmed decays is then more direct.

Note that the FA is expected to break down for charmed nonleptonic B meson decays [19]. The FA holds for charmless decays because of the color transparency argument: contributions from the dominant soft region cancel between the two nonfactorizable diagrams, where the exchanged gluons attach to the quark and the antiquark of the light meson emitted from the weak vertex. For charmed decays with the light meson replaced by a $D^{(*)}$ meson, the two nonfactorizable amplitudes do not cancel due to the mass difference between the two constituent quarks of the $D^{(*)}$ meson. Hence, nonfactorizable contributions ought to be important. This observation leads further to the speculation that strong

*Electronic address: yykeum@eken.phys.nagoya-u.ac.jp
†Electronic address: krmt@k2.sci.toyama-u.ac.jp
‡Electronic address: hnli@phys.sinica.edu.tw
§Electronic address: lucd@ihep.ac.cn
‖Electronic address: sanda@eken.phys.nagoya-u.ac.jp
¶Mailing address.

phases in the $B \to D^{(*)}M$ decays, if there are any, arise from nonfactorizable amplitudes. In charmless decays, strong phases come from annihilation amplitudes through the $(S+P)(S-P)$ penguin operators, since nonfactorizable ones are negligible as explained above. Annihilation amplitudes should not be the source of strong phases for charmed decays, which do not involve the $(S+P)(S-P)$ penguin operators.

In this paper we shall apply the PQCD formalism to the two-body charmed decays $B \to D^{(*)}M$ with $M = \pi$, ρ, and ω. PQCD has predicted strong phases from the annihilation amplitudes for charmless decays that are consistent with the recently measured CP asymmetries in the $B_d^0 \to \pi^+ \pi^-$ modes. It is then interesting to examine whether PQCD also gives the correct magnitude and strong phases from the non-factorizable amplitudes implied by the isospin relation of the $B \to D^{(*)}M$ decays. Compared to the work in [11], the contributions from the twist-3 light meson distribution amplitudes and the threshold resummation effect have been taken into account, and more modes analyzed. The power counting rules for charmed B meson decays, constructed in [20], are employed to obtain the leading factorization formulas. It will be shown that nonfactorizable contributions to charmed decays are calculable in PQCD, and play an important role in explaining the isospin relation indicated by experimental data. The predictions for the $B \to D^{*0}\rho^0, D^{*0}\omega$ branching ratios can be confronted with future measurements.

In Sec. II we review the progress in the study of two-body charmed nonleptonic B meson decays in the literature. The PQCD analysis of the above decays is presented in Sec. III by taking the $B \to D\pi$ modes as an example. Numerical results for all the $B \to D^{(*)}M$ branching ratios and for the extracted BSW parameters a_1 and a_2 are collected in Sec. IV. In Sec. V we compare the PQCD approach to exclusive B meson decays with others in the literature. Section VI is the conclusion. The Appendix contains the explicit expressions of the factorization formulas.

II. REVIEW OF PREVIOUS WORKS

A. PQCD approach to $B \to D^{(*)}$ form factors

To develop the PQCD formalism for charmed B meson decays, we have investigated the $B \to D^{(*)}$ transition form factors in the large recoil region of the $D^{(*)}$ meson [20]. We briefly review this formalism, which serves as the basis of the $B \to D^{(*)}M$ analysis. The $B \to D^{(*)}$ transition is more complicated than the $B \to \pi$ one, because it involves three scales: the B meson mass m_B, the $D^{(*)}$ meson mass $m_{D(*)}$, and the heavy meson and heavy quark mass difference $\bar{\Lambda} = m_B - m_b \sim m_{D(*)} - m_c$ of the order of the QCD scale Λ_{QCD}, $m_{D(*)}$ (m_c) being the $D^{(*)}$ meson (c quark) mass. We have postulated the hierarchy of the three scales

$$m_B \gg m_{D(*)} \gg \bar{\Lambda}, \tag{1}$$

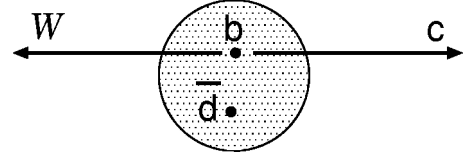which allows a consistent power expansion in $m_{D(*)}/m_B$ and in $\bar{\Lambda}/m_{D(*)}$.

FIG. 1. $B \to D^{(*)}$ transition through b quark decay into a c quark and a virtual W boson.

We write the B ($D^{(*)}$) meson momentum P_1 (P_2) in the light-cone coordinates as

$$P_1 = \frac{m_B}{\sqrt{2}}(1,1,\mathbf{0}_T), \quad P_2 = \frac{m_B}{\sqrt{2}}\left(1, \frac{m_{D(*)}^2}{m_B^2}, \mathbf{0}_T\right). \tag{2}$$

The picture associated with the $B \to D^{(*)}$ transition is shown in Fig. 1, where the initial state is approximated by the $b\bar{d}$ component. The b quark decays into a c quark and a virtual W boson, which carries the momentum q. Since the constituents are roughly on the mass shell, we have the invariant masses $k_i^2 \sim O(\bar{\Lambda}^2)$, $i = 1$ and 2, where k_1 (k_2) is the momentum of the spectator $\bar{d}$ quark in the B ($D^{(*)}$) meson. The above kinematic constraints lead to the order of magnitude of k_1 and k_2 [20]

$$k_1^\mu \sim (\bar{\Lambda}, \bar{\Lambda}, \bar{\Lambda}),$$

$$k_2^\mu \sim \left(\frac{m_B}{m_{D(*)}}\bar{\Lambda}, \frac{m_{D(*)}}{m_B}\bar{\Lambda}, \bar{\Lambda}\right). \tag{3}$$

The lowest-order diagrams contributing to the $B \to D^{(*)}$ form factors contain a hard gluon exchange between the b or c quark and the $\bar{d}$ quark as shown in Fig. 2. The $\bar{d}$ quark undergoes scattering in order to catch up with the c quark, forming a $D^{(*)}$ meson. With the parton momenta in Eq. (3), the exchanged gluon is off shell by

$$(k_1 - k_2)^2 \sim -\frac{m_B}{m_{D(*)}}\bar{\Lambda}^2, \tag{4}$$

which has been identified as the characteristic scale of the hard kernels. From Eq. (1), we have $m_B/m_D^{(*)} \gg 1$, and the hard kernels are calculable in perturbation theory. It has been
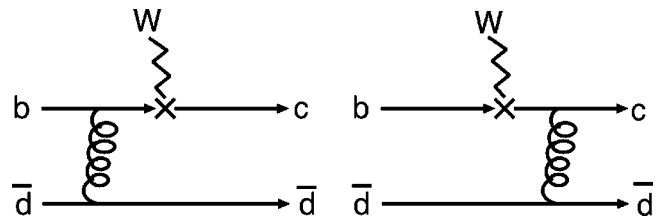

FIG. 2. Lowest-order diagrams contributing to the $B \to D^{(*)}$ form factors. Quite a lot of momentum must be transferred to the spectator $\bar{d}$ quark through the hard gluon exchange.

found that the applicability of PQCD to the $B \to D^{(*)}$ transition at large recoil is marginal for the physical masses m_B and $m_{D^{(*)}}$ [20].

Infrared divergences arise from higher-order corrections to Fig. 2. The soft (collinear) type of divergence is absorbed into the B $(D^{(*)})$ meson wave function $\phi_B(x_1, b_1)$ $[\phi_{D^{(*)}}(x_2, b_2)]$, which is not calculable but universal. The impact parameter b_1 (b_2) is conjugate to the transverse momentum k_{1T} (k_{2T}) carried by the $\bar{d}$ quark in the B $(D^{(*)})$ meson. It has been shown, from the equations of motion for the relevant nonlocal matrix elements, that $\phi_B(x_1, b_1)$ $[\phi_{D^{(*)}}(x_2, b_2)]$ has a peak at the momentum fraction $x_1 \equiv k_1^-/P_1^- \sim \bar{\Lambda}/m_B$ $(x_2 \equiv k_2^+/P_2^+ \sim \bar{\Lambda}/m_{D^{(*)}})$ [20].

The form factors are then expressed as the convolution of the hard kernels H with the B and $D^{(*)}$ meson wave functions in the k_T factorization theorem,

$$F^{BD^{(*)}}(q^2) = \int dx_1 dx_2 d^2 b_1 d^2 b_2 \, \phi_B(x_1, b_1)$$

$$\times H(x_1, x_2, b_1, b_2) \phi_{D^{(*)}}(x_2, b_2). \quad (5)$$

The $D^{(*)}$ meson wave function contains a Sudakov factor arising from k_T resummation, which sums the large double logarithms $\alpha_s \ln^2(m_B b_2)$ to all orders. The B meson wave function also contains such a Sudakov factor, whose effect is negligible because a B meson is dominated by soft dynamics. The hard kernels involve a Sudakov factor from threshold resummation, which sums the large double logarithm $\alpha_s \ln^2 x_1$ or $\alpha_s \ln^2 x_2$ to all orders. This factor modifies the end-point behavior of the B and $D^{(*)}$ meson wave functions effectively, causing them to diminish faster in the small-$x_{1,2}$ region.

B. End-point singularity and Sudakov factor

It has been pointed out that if Fig. 2 is evaluated in the collinear factorization theorem, an end-point singularity appears [21]. In this theorem we have the lowest-order hard kernel

$$H^{(0)}(x_1, x_2) \propto \frac{1}{x_1 x_2^2}, \quad (6)$$

from the left diagram in Fig. 2, which leads to a logarithmic divergence, as the $D^{(*)}$ meson distribution amplitude behaves like $\phi_{D^{(*)}}(x_2) \propto x_2$ in the small-x_2 region. This singularity implies the breakdown of collinear factorization, and k_T factorization becomes more appropriate. Once the parton transverse momenta k_T are taken into account, Eq. (6) is modified into

$$H^{(0)}(x_1, x_2, \mathbf{k}_{1T}, \mathbf{k}_{2T})$$

$$\propto \frac{m_B^4}{[x_1 x_2 m_B^2 + (\mathbf{k}_{1T} - \mathbf{k}_{2T})^2][x_2 m_B^2 + \mathbf{k}_{2T}^2]}. \quad (7)$$
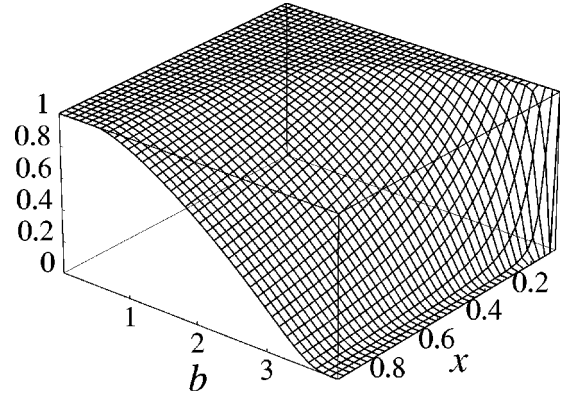

FIG. 3. QCD demands the presence of a Sudakov factor, which is the amplitude for a quark-antiquark color dipole not to emit real gluons in the final state. For a large transverse separation b, the quark and the antiquark do not shield each other's color charge and are likely to radiate. In this region Sudakov suppression is strong.

A dynamical effect, the so-called Sudakov suppression, favors the configuration in which k_T is not small [8]. The end-point singularity then disappears as explained below.

When an electron undergoes harder scattering, it tends to radiate more photons. Hence, the scattering amplitude for radiating no photons must be suppressed by a factor whose effect increases with the electron energy. In QED this is the well-known Sudakov suppression factor, the amplitude for an electron not to emit a photon in hard scattering. In the current QCD case of the $B \to D^{(*)}$ transition, it is the c-$\bar{d}$ quark-antiquark color dipole that undergoes hard scattering. When the color dipole is larger, it tends to radiate more gluons. Since the final state contains only a single $D^{(*)}$ meson, real gluon emission is forbidden in the hard decay process. Similarly, the transition amplitude must involve a Sudakov factor, whose effect increases with the size of the color dipole, i.e., with the separation b between c and $\bar{d}$. That is, a configuration with a smaller separation b or with a larger relative transverse momentum k_T is preferred in the $B \to D^{(*)}$ transition at large recoil. Then the virtual particles involved in the hard kernel remain sufficiently off shell, and Eq. (5), with Eq. (7) inserted, is free from the end-point singularity.

The corresponding Sudakov factor can be derived in PQCD as a function of the transverse separation b and of the momentum fraction x carried by the spectator quark [9], whose behavior is shown in Fig. 3. The Sudakov factor suppresses the large-b region, where the quark and the antiquark are separated by a large transverse distance and the color shielding is not effective. It also suppresses the $x \sim 1$ region, where a quark carries all of the meson momentum and tends to emit real gluons in hard scattering. The Sudakov factors from k_T resummation [22] for the B and $D^{(*)}$ mesons are associated with only light spectator quarks, since the double logarithms arise from the overlap of the soft and mass (collinear) divergences. These factors, being universal, are the same as in all our previous analyses.

Similarly, the small-x region corresponds to a configuration with a soft spectator, i.e., with a large color dipole in the

longitudinal direction. The probability for this large color dipole not to radiate in hard scattering is also described by a Sudakov factor, which comes from threshold resummation for the hard kernels. For the derivation of this Sudakov factor, refer to [23]. For convenience, it has been parametrized as [24]

$$S_t(x) = \frac{2^{1+2c}\Gamma(3/2+c)}{\sqrt{\pi}\Gamma(1+c)}[x(1-x)]^c, \quad (8)$$

with the constant $c = 0.35$. The above parametrization is motivated by the qualitative behavior of S_t: $S_t(x) \rightarrow 0$ as $x \rightarrow 0,1$ [23]. Since threshold resummation is associated with the hard kernels, the result could be process dependent. It has been observed [25] that its effect is essential for factorizable decay topologies and negligible for nonfactorizable decay topologies.

C. Factorization assumption

We review the basics of the FA for the $B \rightarrow D^{(*)}M$ decays. The relevant effective weak Hamiltonian is given by

$$\mathcal{H}_{\text{eff}} = \frac{G_F}{\sqrt{2}}V_{cb}V_{ud}^*[C_1(\mu)O_1(\mu) + C_2(\mu)O_2(\mu)], \quad (9)$$

where the four-fermion operators are

$$O_1 = (\bar{d}b)_{V-A}(\bar{c}u)_{V-A}, \quad O_2 = (\bar{c}b)_{V-A}(\bar{d}u)_{V-A}, \quad (10)$$

with the definition $(\bar{q}_1 q_2)_{V-A} \equiv \bar{q}_1 \gamma_\mu(1-\gamma_5)q_2$, the V's the Cabibbo-Kobayashi-Maskawa (CKM) matrix elements, and C_1 and C_2 the Wilson coefficients. The $\bar{B}^0 \rightarrow D^+\pi^-$ mode is referred to as the class-1 (color-allowed) topology, in which the charged pion is emitted at the weak vertex. The $\bar{B}^0 \rightarrow D^0\pi^0$ mode is referred to as the class-2 (color-suppressed) topology, in which the D^0 meson is directly produced.

For the $\bar{B}^0 \rightarrow D^+\pi^-$ mode, O_2 and a Fierz transformed O_1 contribute. For the $\bar{B}^0 \rightarrow D^0\pi^0$ mode, O_1 and a Fierz transformed O_2 contribute. Applying the FA [1] or generalized[1] FA [2–4] to the hadronic matrix elements, we have

$$\langle D^+\pi^-|(\bar{c}b)_{V-A}(\bar{d}u)_{V-A}|\bar{B}^0\rangle$$

$$\approx \langle D^+|(\bar{c}b)_{V-A}|\bar{B}^0\rangle\langle\pi^-|(\bar{d}u)_{V-A}|0\rangle,$$

$$\langle D^0\pi^0|(\bar{d}b)_{V-A}(\bar{c}u)_{V-A}|\bar{B}^0\rangle$$

$$\approx \langle\pi^0|(\bar{d}b)_{V-A}|\bar{B}^0\rangle\langle D^0|(\bar{c}u)_{V-A}|0\rangle. \quad (11)$$

Substituting the definition of the B meson transition form factors F^{BD} and $F^{B\pi}$ and of the meson decay constants f_π

---

[1]The main difference between the FA and generalized FA is that nonfactorizable contributions are included in the latter.

and f_D, the $\bar{B}^0 \rightarrow D^+\pi^-$ (class-1) and $\bar{B}^0 \rightarrow D^0\pi^0$ (class-2) decay amplitudes are expressed as

$$A(\bar{B}^0 \rightarrow D^+\pi^-) = i\frac{G_F}{\sqrt{2}}V_{cb}V_{ud}^*(m_B^2 - m_D^2)$$

$$\times f_\pi F^{BD}(m_\pi^2)a_1(D\pi), \quad (12)$$

$$\sqrt{2}A(\bar{B}^0 \rightarrow D^0\pi^0) = -i\frac{G_F}{\sqrt{2}}V_{cb}V_{ud}^*(m_B^2 - m_\pi^2)$$

$$\times f_D F^{B\pi}(m_D^2)a_2(D\pi), \quad (13)$$

where the parameters a_1 and a_2 are defined by

$$a_1 = C_2(\mu) + \frac{C_1(\mu)}{N_c}, \quad a_2 = C_1(\mu) + \frac{C_2(\mu)}{N_c}, \quad (14)$$

N_c being the number of colors. The $B^- \rightarrow D^0\pi^-$ mode, involving both classes of amplitudes, is referred to as class 3. The isospin symmetry implies

$$A(\bar{B}^0 \rightarrow D^+\pi^-) = A(B^- \rightarrow D^0\pi^-) + \sqrt{2}A(\bar{B}^0 \rightarrow D^0\pi^0). \quad (15)$$

It is straightforward to apply the FA to other $\bar{B} \rightarrow D^{(*)}M$ modes. a_1 and a_2 depend on the color and Dirac structures of the operators, but otherwise are postulated to be universal [1,26,27]. They have the orders of magnitude $a_1(D\pi) \sim O(1)$ and $a_2(D\pi) \sim O(1/N_c)$. The consistency of the FA can be tested by comparing a_1 and a_2 extracted from various decays. Within errors, the class-1 decays $\bar{B}^0 \rightarrow D^{(*)+}M^-$ with $M = \pi, \rho, a_1, D_s$, and D_s^* are described using a universal value $|a_1| \approx 1.1 \pm 0.1$, whereas the class-2 decays $\bar{B} \rightarrow \bar{K}^{(*)}M$ with $M = J/\psi$ and $\psi(2S)$ suggest a nearly universal value $|a_2| \approx 0.2$–0.3 [28]. The wide range of $|a_2|$ is due to the uncertainty in the $B \rightarrow K^{(*)}$ form factors. The class-3 decays $B^- \rightarrow D^{(*)0}M^-$ with $M = \pi$ and ρ, which are sensitive to the interference of the two decay topologies, can be explained by a real and positive ratio $a_2/a_1 \approx 0.2$–0.3, which seems to agree with the above determination of $|a_1|$ and $|a_2|$. This is the reason the FA was claimed to work well in explaining two-body charmed B meson decays, before the class-2 modes $\bar{B}^0 \rightarrow D^0M^0$ with $M = \pi, \eta$, and ω were measured.

The recently observed $\bar{B}^0 \rightarrow D^0M^0$ branching ratios listed in Table I [29,30] revealed interesting QCD dynamics. The parameter $|a_2|$ directly extracted from these modes falls into the range of $|a_2(D\pi)| \sim 0.35$–0.60 and $|a_2(D^*\pi)| \sim 0.25$–0.50 [31]. To maintain the predictions for the class-3 decays, there must exist sizable strong phases between class-1 and class-2 amplitudes [19], which are $\text{Arg}(a_2/a_1) = 59°$ for the $D\pi$ modes and $\text{Arg}(a_2/a_1) = 63°$ for the $D^*\pi$ modes [31]. These results can be regarded as a failure of the FA: the parameters a_2 in different types of decays, such as $\bar{B} \rightarrow D^{(*)}\pi$ and $\bar{B} \rightarrow \bar{K}^{(*)}J/\psi$, differ by almost a factor of 2 in magnitude, implying strong nonuniversal nonfactorizable

TABLE I. Data (in units of 10^{-4}) of the $\bar{B}^0 \to D^{(*)0} M^0$ ($M^0 = \pi, \eta, \omega$) branching ratios.

Decay mode	Belle [29]	CLEO [30]
$\bar{B}^0 \to D^0 \pi^0$	$3.1 \pm 0.4 \pm 0.5$	$2.74^{+0.36}_{-0.32} \pm 0.55$
$\bar{B}^0 \to D^{*0} \pi^0$	$2.7^{+0.8+0.5}_{-0.7-0.6}$	$2.20^{+0.59}_{-0.52} \pm 0.79$
$\bar{B}^0 \to D^0 \eta$	$1.4^{+0.5}_{-0.4} \pm 0.3$	
$\bar{B}^0 \to D^{*0} \eta$	$2.0^{+0.9}_{-0.8} \pm 0.4$	
$\bar{B}^0 \to D^0 \omega$	$1.8 \pm 0.5^{+0.4}_{-0.3}$	
$\bar{B}^0 \to D^{*0} \omega$	$3.1^{+1.3}_{-1.1} \pm 0.8$	

effects. It is then crucial to understand this nonuniversality and, especially, the mechanism responsible for the large relative phases in a systematic QCD framework.

III. $B \to D\pi$ IN PQCD

In this section we take the $B \to D\pi$ decays as an example of the PQCD analysis. An intensive study of all other modes will be performed in the next section. The $B \to D\pi$ decay rates have the expressions

$$\Gamma_i = \frac{1}{128\pi} G_F^2 |V_{cb}|^2 |V_{ud}|^2 \frac{m_B^3}{r} |A_i|^2. \tag{16}$$

The indices for the classes $i = 1$, 2, and 3, denote the modes $\bar{B}^0 \to D^+ \pi^-$, $\bar{B}^0 \to D^0 \pi^0$, and $B^- \to D^0 \pi^-$, respectively. The amplitudes A_i are written as

$$A_1 = f_\pi \xi_{\text{ext}} + f_B \xi_{\text{exc}} + \mathcal{M}_{\text{ext}} + \mathcal{M}_{\text{exc}}, \tag{17}$$

$$\sqrt{2} A_2 = -(f_D \xi_{\text{int}} - f_B \xi_{\text{exc}} + \mathcal{M}_{\text{int}} - \mathcal{M}_{\text{exc}}), \tag{18}$$

$$A_3 = f_\pi \xi_{\text{ext}} + f_D \xi_{\text{int}} + \mathcal{M}_{\text{ext}} + \mathcal{M}_{\text{int}}, \tag{19}$$

with f_B being the B meson decay constant. The functions ξ_{ext}, ξ_{int}, and ξ_{exc} denote the factorizable external W-emission (color-allowed), internal W-emission (color-suppressed), and W-exchange contributions, which come from Figs. 4(a) and 4(b), Figs. 5(a) and 5(b), and Figs. 6(a) and 6(b), respectively. The functions $\mathcal{M}_{\text{ext}}$, $\mathcal{M}_{\text{int}}$, and $\mathcal{M}_{\text{exc}}$ represent the nonfactorizable external W-emission, internal W-emission, and W-exchange contributions, which come from Figs. 4(c) and 4(d), Figs. 5(c) and 5(d), and Figs. 6(c) and 6(d), respectively. All the topologies, including the factorizable and nonfactorizable ones, have been taken into account. It is easy to find that Eqs. (17)–(19) obey the isospin relation in Eq. (15).

In the PQCD framework based on the k_T factorization theorem, an amplitude is expressed as the convolution of

hard b quark decay kernels with meson wave functions in both the longitudinal momentum fractions and the transverse momenta of partons. Our PQCD formulas are derived up to leading order in α_s, to leading power in m_D/m_B and in $\bar{\Lambda}/m_D$, and to leading double-logarithm resummations. For the Wilson coefficients, we adopt the leading-order renormalization-group evolution for consistency, although the next-to-leading-order ones are available in the literature [32]. For a similar reason, we employ the one-loop running coupling constant $\alpha_s(\mu) = 2\pi/[\beta_1 \ln(\mu/\Lambda_{\text{QCD}}^{(n_f)})]$ with $\beta_1 = (33 - 2n_f)/3$, n_f being the number of active quarks. The QCD scale is chosen as $\Lambda_{\text{QCD}}^{(5)} = 193$ MeV for the scale $m_b < \mu < m_W$, which is derived from $\Lambda_{\text{QCD}}^{(4)} = 250$ MeV for $\mu < m_b$.

The leading-order and leading-power factorization formulas for the above decay amplitudes are collected in the Appendix. Here we mention only some key ingredients in the calculation. The formulas for the $B \to D\pi$ decays turn out to be simpler than those for the $B \to \pi\pi$ ones. The simplicity is attributed to the power counting rules under the hierarchy of the three scales in Eq. (1). The hard kernels are evaluated up to power corrections of order $\bar{\Lambda}/m_D \sim m_D/m_B$ ($\bar{\Lambda}/m_B$ is regarded as being of even higher power). Following these rules, the terms proportional to $x_1 \sim \bar{\Lambda}/m_B$ and to $x_2 \sim \bar{\Lambda}/m_D$ are of higher power compared to the leading $O(1)$ terms and are dropped. We have also dropped the terms of higher powers in $r = m_D/m_B$. Accordingly, the phase space factor $1 - r^2$, appearing in Eq. (16) originally, has been approximated by 1. This approximation is irrelevant in explaining the ratios of the $B \to D\pi$ branching ratios, and causes an uncertainty in the absolute branching ratios that is much smaller than those from the CKM matrix element $|V_{cb}|$ and from the meson decay constants f_B and f_D.

Up to power corrections of order $\bar{\Lambda}/m_B$ and $\bar{\Lambda}/m_D$, we consider only a single B (D) meson wave function. The nonperturbative B meson and pion wave functions were fixed in our previous work [14,15]. The unknown D meson wave function was determined by fitting the PQCD predictions for the $B \to D$ transition form factors to the observed $B \to Dl\nu$ decay spectrum [20]. The contributions from the two-parton twist-3 D meson wave functions, being of higher power, are negligible. Note that in charmless decays the contributions from the two-parton twist-3 light meson distribution amplitudes are not down by a power of $1/m_B$. These distribution amplitudes, being constant at the momentum fraction $x \to 0$ as required by the equations of motion, lead to linear singularities in the collinear factorization formulas. The linear singularities modify the naive power counting, such that two-parton twist-3 contributions become leading power [24,33]. In charmed decays the above equations of motion are modi-
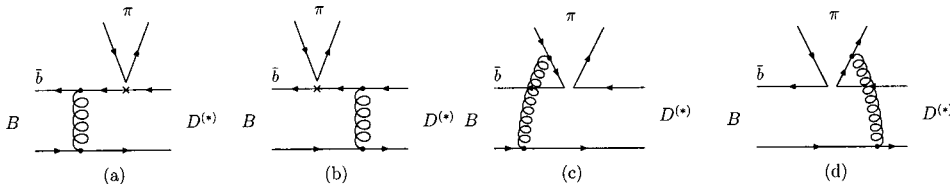
FIG. 4. Color-allowed emission diagrams contributing to the $B \to D^{(*)} \pi$ decays.

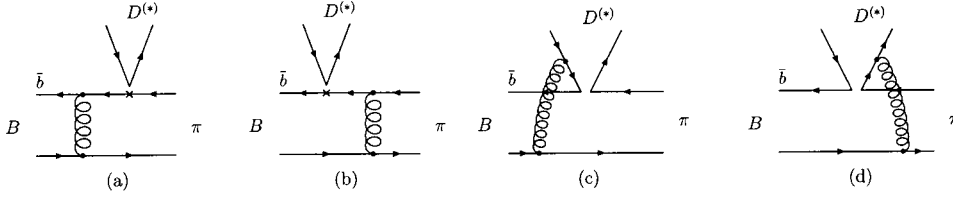FIG. 5. Color-suppressed emission diagrams contributing to the $B \to D^{(*)}\pi$ decays.

fied [20], and the two-parton twist-3 D meson wave functions vanish at the end point of x. Therefore, their contributions are indeed of higher power.

Retaining the parton transverse momenta k_T, the nonfactorizable topologies generate strong phases from non pinched singularities of the hard kernels [34]. For example, the virtual quark propagator in Fig. 5(d) is written, in the principal-value prescription, as

$$\frac{1}{x_3(x_2-x_1)m_B^2 - (\mathbf{k}_{2T} - \mathbf{k}_{1T} + \mathbf{k}_{3T})^2 + i\epsilon}$$

$$= P\left[\frac{1}{x_3(x_2-x_1)m_B^2 - (\mathbf{k}_{2T} - \mathbf{k}_{1T} + \mathbf{k}_{3T})^2}\right]$$

$$- i\pi\delta(x_3(x_2-x_1)m_B^2 - (\mathbf{k}_{2T} - \mathbf{k}_{1T} + \mathbf{k}_{3T})^2), \quad (20)$$

with x_3 being the momentum fraction associated with the pion. The second term contributes to the strong phase, which is thus of short-distance origin and calculable. The first term in the above expression does not lead to an end-point singularity. Note that the strong phase from Eq. (20) is obtained by keeping all terms in the denominator of a propagator without neglecting x_1 and x_2.

IV. NUMERICAL RESULTS

The computation of the hard kernels in the k_T factorization theorem for other charmed decay modes is similar and straightforward. The $B \to D^*\pi$ decay amplitudes are the same as the $B \to D\pi$ ones but with the substitution of the mass, the decay constant, and the distribution amplitude,

$$m_D \to m_{D*}, \quad f_D \to f_{D*}, \quad \phi_D(x_2) \to \phi_{D*}(x_2). \quad (21)$$

This simple substitution is expected at leading power under the hierarchy in Eq. (1): the difference between the two channels should occur only at $O(\bar{\Lambda}/m_D)$. An explicit derivation shows that the difference occurs at the twist-3 level for the nonfactorizable emission diagrams in Fig. 4 and for the annihilation diagrams in Fig. 6. It implies that the universal-

ity (channel independence) of a_1 and a_2 assumed in the FA [35] breaks down at subleading power even within the $B \to D^{(*)}M$ decays.

Replacing the pion in Figs. 4–6 by the ρ (ω) meson, we obtain the diagrams for the $B \to D^{(*)}\rho(\omega)$ decays. The factorization formulas for the $B \to D\rho(\omega)$ decay amplitudes are also the same as those for the $B \to D\pi$ ones but with the substitutions

$$\phi_\pi \to \phi_{\rho,\omega}, \quad \phi_\pi^p \to \phi_{\rho,\omega}^s, \quad \phi_\pi^t \to \phi_{\rho,\omega}^t, \quad m_0 \to m_{\rho(\omega)},$$
$$(22)$$

where ϕ_π ($\phi_\pi^{p,t}$) is the two-parton twist-2 (twist-3) pion distribution amplitude, $\phi_{\rho,\omega}$ ($\phi_{\rho,\omega}^{s,t}$) the two-parton twist-2 (twist-3) ρ and ω meson distribution amplitudes, respectively, m_0 the chiral enhancement scale, and $m_{\rho(\omega)}$ the ρ (ω) meson mass. Hence, a similar isospin relation holds:

$$A(B^0 \to D^-\rho^+) = A(B^+ \to \bar{D}^0\rho^+) + \sqrt{2}A(B^0 \to \bar{D}^0\rho^0).$$
$$(23)$$

The $B \to D^*\rho(\omega)$ decays contain more amplitudes associated with the different polarizations. However, at leading power, the amplitudes associated with the transverse polarizations, suppressed by a power of m_{D*}/m_B or of m_ρ/m_B, are negligible. That is, the factorization formulas for the $B \to D^*\rho(\omega)$ modes are the same as the $B \to D\rho(\omega)$ ones with the substitution in Eq. (21). Note that the W-exchange contribution changes sign in the $\bar{B}^0 \to D^{(*)0}\omega$ decay amplitude:

$$A(\bar{B}^0 \to D^{(*)0}\omega) = -\frac{1}{\sqrt{2}}(f_{D^{(*)}}\xi_{\text{int}} + f_B\xi_{\text{exc}} + \mathcal{M}_{\text{int}} + \mathcal{M}_{\text{exc}}),$$
$$(24)$$

due to the different quark structures between the ω meson (proportional to $u\bar{u} + d\bar{d}$) and the ρ^0 meson (proportional to $u\bar{u} - d\bar{d}$).

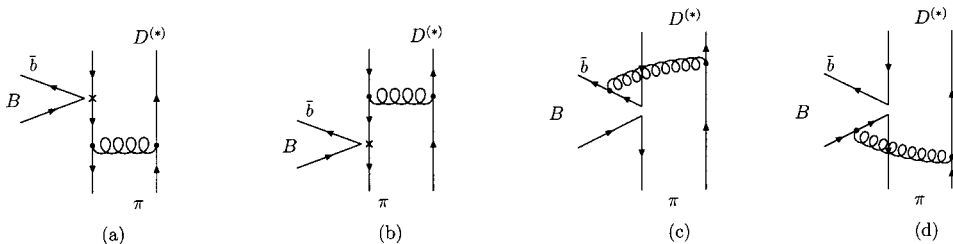In the numerical analysis we adopt the model for the B meson wave function

FIG. 6. Annihilation diagrams contributing to the $B \to D^{(*)}\pi$ decays.

TABLE II. Predicted $B \rightarrow D\pi$ decay amplitudes in units of 10^{-2} GeV.

Amplitudes	$C_D = 0.6$	$C_D = 0.8$	$C_D = 1.0$
$f_\pi \xi_{\text{ext}}$	6.90	7.46	8.01
$f_D \xi_{\text{int}}$	-1.44	-1.44	-1.44
$f_B \xi_{\text{exc}}$	$-0.01 - 0.03i$	$-0.02 - 0.03i$	$-0.02 - 0.03i$
$\mathcal{M}_{\text{ext}}$	$-0.24 + 0.57i$	$-0.25 + 0.60i$	$-0.27 + 0.65i$
$\mathcal{M}_{\text{int}}$	$3.34 - 3.02i$	$3.22 - 3.07i$	$3.10 - 3.12i$
$\mathcal{M}_{\text{exc}}$	$-0.26 - 0.89i$	$-0.31 - 0.95i$	$-0.37 - 1.02i$

$$\phi_B(x,b) = N_B x^2 (1-x)^2 \exp\left[-\frac{1}{2}\left(\frac{xm_B}{\omega_B}\right)^2 - \frac{\omega_B^2 b^2}{2} \right],$$
(25)

with the shape parameter ω_B and the normalization constant N_B being related to the decay constant f_B through

$$\int dx \, \phi_B(x,0) = \frac{f_B}{2\sqrt{2N_c}}.$$
(26)

The $D^{(*)}$ meson distribution amplitude is given by

$$\phi_{D^{(*)}}(x) = \frac{3}{\sqrt{2N_c}} f_{D^{(*)}} x(1-x)[1 + C_{D^{(*)}}(1-2x)],$$
(27)

with the shape parameter $C_{D^{(*)}}$. The pion and $\rho(\omega)$ meson distribution amplitudes have been derived in [36,37], and their explicit expressions are given in the Appendix. The B meson wave function was then extracted from the light-cone-sum-rule (LCSR) results for the $B \rightarrow \pi$ transition form factor [24]. The range of $C_{D^{(*)}}$ was determined from the measured $B \rightarrow D^{(*)} l\nu$ decay spectrum at large recoil by employing the B meson wave function extracted above. We do not consider the variation of $\phi_{D^{(*)}}$ with the impact parameter b, since the available data are not yet sufficiently precise to control this dependence.

The input parameters are listed below:

$$f_B = 190 \text{ MeV}, \quad \omega_B = 0.4 \text{ GeV},$$

$$f_D = 240 \text{ MeV}, \quad C_D = 0.8 \pm 0.2,$$

$$f_{D*} = 230 \text{ MeV}, \quad C_{D*} = 0.7 \pm 0.2,$$

$$f_\pi = 132 \text{ MeV}, \quad f_\rho = f_\omega = 200 \text{ MeV},$$

$$f_\rho^T = f_\omega^T = 160 \text{ MeV}, \quad m_B = 5.28 \text{ GeV},$$

$$m_b = 4.8 \text{ GeV}, \quad m_D = 1.87 \text{ GeV},$$

$$m_{D*} = 2.01 \text{ GeV}, \quad m_c = 1.3 \text{ GeV},$$

$$m_\rho = 0.77 \text{ GeV}, \quad m_\omega = 0.78 \text{ GeV},$$

$$m_t = 170 \text{ GeV}, \quad m_W = 80.41 \text{ GeV},$$

$$m_0 = 1.4 \text{ GeV}, \quad \tau_{B^\pm} = 1.674 \times 10^{-12} \text{ s},$$

$$\tau_{B^0} = 1.542 \times 10^{-12} \text{ s},$$

$$G_F = 1.16639 \times 10^{-5} \text{ GeV}^{-2},$$

$$|V_{cb}| = 0.043, \quad |V_{ud}| = 0.974,$$
(28)

where m_t, m_W, $\tau_{B^\pm}$, and τ_{B^0} denote the top quark mass, the W boson mass, the $B^\pm$ meson lifetime, and the B^0 meson lifetime, respectively. The above meson wave functions and parameters correspond to the form factors at maximal recoil

$$F_0^{B\pi} \sim 0.3, \quad \xi_+^{BD} \sim 0.57, \quad \xi_{A_1}^{BD*} \sim 0.52,$$
(29)

which are close to the results from QCD sum rules [38,39]. We stress that there is no arbitrary parameter in our calculation, although the value of each parameter is known only up to a range.

The PQCD predictions for each term of the $B \rightarrow D\pi$ decay amplitudes are exhibited in Table II. The theoretical uncertainty comes only from the variation of the shape parameter for the D meson distribution amplitude, $0.6 < C_D < 1.0$. It is expected that the color-allowed factorizable amplitude $f_\pi \xi_{\text{ext}}$ dominates, and that the color-suppressed factorizable contribution $f_D \xi_{\text{int}}$ is smaller due to the Wilson coefficient $C_1 + C_2/N_c \sim 0$. The color-allowed nonfactorizable amplitude $\mathcal{M}_{\text{ext}}$ is negligible: since the pion distribution amplitude is symmetric under the exchange of x_3 and $1 - x_3$, the contributions from the two diagrams Figs. 4(c) and 4(d) cancel each other in the dominant region with small x_2. It is also down by the small Wilson coefficient C_1/N_c. For the color-suppressed nonfactorizable contribution $\mathcal{M}_{\text{int}}$, the above cancellation does not exist in the dominant region with small x_3, because the D meson distribution amplitude $\phi_D(x_2)$ is not symmetric under the exchange of x_2 and $1 - x_2$. Furthermore, $\mathcal{M}_{\text{int}}$, proportional to $C_2/N_c \sim 0.3$, is not down by the Wilson coefficient. It is indeed comparable to the color-allowed factorizable amplitude $f_\pi \xi_{\text{ext}}$, and produces a large strong phase as explained in Eq. (20). Both the factorizable and nonfactorizable annihilation contributions are small, consistent with our argument in Sec. II.

The predicted branching ratios in Table III are in agreement with the averaged experimental data [29,30,40]. We extract the parameters a_1 and a_2 by equating Eqs. (12) and (13) to Eqs. (17) and (18), respectively. That is, our a_1 and a_2 contain not only the nonfactorizable amplitudes as in the

TABLE III. Predicted $B \rightarrow D\pi$ decay amplitudes in units of 10^{-2} GeV, branching ratios in units of 10^{-3}, $|a_2/a_1|$, and relative angle $\mathrm{Arg}(a_2/a_1)$ in degrees.

Quantities	$C_D = 0.6$	$C_D = 0.8$	$C_D = 1.0$	Data
A_1	$6.39 - 0.35i$	$6.88 - 0.38i$	$7.35 - 0.40i$	
A_2	$-1.53 + 1.48i$	$-1.49 + 1.48i$	$-1.45 + 1.45i$	
A_3	$8.56 - 2.45i$	$8.99 - 2.47i$	$9.40 - 2.46i$	
$B(\bar{B}^0 \rightarrow D^+\pi^-)$	2.37	2.74	3.13	3.0 ± 0.4
$B(\bar{B}^0 \rightarrow D^0\pi^0)$	0.26	0.25	0.24	0.29 ± 0.05
$B(B^- \rightarrow D^0\pi^-)$	4.96	5.43	5.91	5.3 ± 0.5
$|a_2/a_1|$ (without annihilation)	0.47 (0.51)	0.43 (0.46)	0.39 (0.42)	
$\mathrm{Arg}(a_2/a_1)$ (without annihilation)	$-42.5°$ ($-61.5°$)	$-41.6°$ ($-63.5°$)	$-41.9°$ ($-65.3°$)	

generalized FA, but also the small annihilation amplitudes, as was first discussed in [41]. We obtain the ratio $|a_2/a_1|$ ~ 0.43 with 10% uncertainty and the phase of a_2 relative to a_1 about $\mathrm{Arg}(a_2/a_1) \sim -42°$. If the annihilation amplitudes $f_B\xi_{\mathrm{exc}}$ and $\mathcal{M}_{\mathrm{exc}}$ are excluded, we have $|a_2/a_1| \sim 0.46$ and $\mathrm{Arg}(a_2/a_1) \sim -64°$. Note that the experimental data do not fix the sign of the relative phases. The PQCD calculation indicates that $\mathrm{Arg}(a_2/a_1)$ should be located in the fourth quadrant. It is evident that the short-distance strong phase from the color-suppressed nonfactorizable amplitude is already sufficient to account for the isospin triangle formed by the $B \rightarrow D\pi$ modes. The conclusion that the data hint at a large final-state interaction was drawn from an analysis based on the FA [19,31,42,43]. Hence, it is more reasonable to claim that the data just imply a large strong phase, but do not tell what mechanism generates this phase [44]. From the viewpoint of PQCD, this strong phase is of short distance and produced from the nonpinched singularity of the hard kernel. Certainly, under the current experimental and theoretical uncertainties, there is still room for long-distance phases from final-state interaction.

The PQCD predictions for the $B \rightarrow D^*\pi$ decay amplitudes and branching ratios in Table IV are also consistent with the data [45]. Since m_{D*} and ϕ_{D*} are only slightly different from m_D and ϕ_D, respectively, the results are close

to those in Table III. The $B \rightarrow D^*\pi$ branching ratios are smaller than the $B \rightarrow D\pi$ ones because of the form factors $\xi_{A_1}^{BD*} < \xi_+^{BD}$ as shown in Eq. (29). Similarly, the ratio $|a_2/a_1|$ and the relative phase $\mathrm{Arg}(a_2/a_1)$ are also close to those associated with the $B \rightarrow D\pi$ decays. We obtain the ratio $|a_2/a_1| \sim 0.47$ with 10% uncertainty and the relative phase about $\mathrm{Arg}(a_2/a_1) \sim -41°$. Excluding the annihilation amplitudes, we have $|a_2/a_1| \sim 0.5$ and $\mathrm{Arg}(a_2/a_1) \sim -63°$.

The PQCD predictions for the $B \rightarrow D^{(*)}\rho(\omega)$ branching ratios are listed in Table V, which match the data [45]. The $\bar{B}^0 \rightarrow D^+\rho^-$ and $B^- \rightarrow D^0\rho^-$ branching ratios are about twice the $\bar{B}^0 \rightarrow D^+\pi^-$ and $B^- \rightarrow D^0\pi^-$ ones because of the larger ρ meson decay constant, $(f_\rho/f_\pi)^2 \sim 2$. The relatively smaller $\bar{B}^0 \rightarrow D^0\rho^0$ branching ratio is attributed to the cancellation of the above enhancing effect between the color-suppressed and W-exchange contributions, consistent with the observation made in an analysis based on the topological-amplitude parametrization [46]. The $\bar{B}^0 \rightarrow D^0\omega$ branching ratio is larger than the $\bar{B}^0 \rightarrow D^0\rho^0$ one due to the constructive interference between the color-suppressed contribution and the annihilation contribution as indicated in Eq. (24). To obtain the $\bar{B}^0 \rightarrow D^*\rho$ helicity amplitudes and their relative phases [47], the power-suppressed contributions from the

TABLE IV. Predicted $B \rightarrow D^*\pi$ decay amplitudes in units of 10^{-2} GeV, branching ratios in units of 10^{-3}, $|a_2/a_1|$, and relative angle $\mathrm{Arg}(a_2/a_1)$ in degrees.

Quantities	$C_{D*} = 0.5$	$C_{D*} = 0.7$	$C_{D*} = 0.9$	Data
A_1	$6.32 - 0.42i$	$6.81 - 0.45i$	$7.30 - 0.49i$	
A_2	$-1.65 + 1.61i$	$-1.62 + 1.59i$	$-1.59 + 1.57i$	
A_3	$8.65 - 2.69i$	$9.10 - 2.70i$	$9.55 - 2.70i$	
$B(\bar{B}^0 \rightarrow D^{*+}\pi^-)$	2.16	2.51	2.88	2.76 ± 0.21
$B(\bar{B}^0 \rightarrow D^{*0}\pi^0)$	0.29	0.28	0.27	0.25 ± 0.07
$B(B^- \rightarrow D^{*0}\pi^-)$	4.79	5.26	5.75	4.60 ± 0.40
$|a_2/a_1|$ (without annihilation)	0.52 (0.55)	0.47 (0.50)	0.43 (0.47)	
$\mathrm{Arg}(a_2/a_1)$ (without annihilation)	$-40.5°$ ($-61.4°$)	$-40.7°$ ($-63.1°$)	$-40.8°$ ($-64.8°$)	

TABLE V. Predicted $B \to D^{(*)}\rho(\omega)$ branching ratios in units of 10^{-3}.

Branching ratios	$C_D = 0.6$	$C_D = 0.8$	$C_D = 1.0$	Data
$B(\bar{B}^0 \to D^+ \rho^-)$	4.10	4.72	5.38	8.0 ± 1.4
$B(\bar{B}^0 \to D^0 \rho^0)$	0.17	0.17	0.17	0.29 ± 0.11
$B(B^- \to D^0 \rho^-)$	7.26	8.15	9.09	13.4 ± 1.8
$B(\bar{B}^0 \to D^0 \omega)$	0.50	0.54	0.56	0.18 ± 0.06
Branching ratios	$C_{D*} = 0.5$	$C_{D*} = 0.7$	$C_{D*} = 0.9$	Data
$B(\bar{B}^0 \to D^{*+} \rho^-)$	5.32	6.16	7.08	7.3 ± 1.5
$B(\bar{B}^0 \to D^{*0} \rho^0)$	0.18	0.18	0.19	< 0.51
$B(B^- \to D^{*0} \rho^-)$	9.14	10.32	11.60	15.5 ± 3.1
$B(\bar{B}^0 \to D^{*0} \omega)$	0.49	0.53	0.58	< 0.74

transverse polarizations must be included. For consistency, the contribution from the longitudinal polarization should be calculated up to the same power. We shall study this subject in a forthcoming paper. The predictions for the $B \to D^{*0}\rho^0, D^{*0}\omega$ decays can be compared with future measurement. The latter branching ratio is larger than the former for the same reason as for the $B \to D^0\rho^0, D^0\omega$ decays.

V. COMPARISON WITH OTHER APPROACHES

In this section we make a brief comparison of the PQCD formalism with other QCD approaches to exclusive B meson decays, emphasizing the differences. For more details, refer to [48]. As mentioned before, there are two kinds of factorization theorem for QCD processes [13]: collinear factorization, on which the soft-collinear effective theory (SCET) [49,50], LCSR [51,52], and QCDF [5] are based, and k_T factorization, on which the PQCD approach is based. Calculating the $B \to \pi$ form factor $F^{B\pi}$ in collinear factorization up to leading power in $1/m_B$ and leading order in α_s, an endpoint singularity occurs. Hence, we define three types of contributions: a genuine soft contribution f^S, a contribution f^{EP} containing the end-point singularity, and a finite contribution f^F:

$$F^{B\pi} = f^S + f^{EP} + f^F. \qquad (30)$$

The second term cannot cover the complete soft contribution, because it is from a leading formalism. Note that the endpoint singularity exists even in the heavy quark limit. Hence, B meson decays differ from other exclusive processes, which become calculable in collinear factorization at sufficiently large momentum transfer.

There are two options to handle the above end-point singularity [53]. First, an end-point singularity in collinear factorization implies that exclusive B meson decays are dominated by soft dynamics. Therefore, a heavy-to-light form factor is not calculable, and f^{EP} should be treated as a soft object, like f^S. In SCET and QCDF, $F^{B\pi}$ is then written, up to $O(\alpha_s)$, as [54,55]

$$F^{B\pi} = f^{NF} + f^F, \qquad (31)$$

with

$$f^{NF} = f^S + f^{EP},$$

$$f^F = \phi_B \otimes T' \otimes \phi_\pi. \qquad (32)$$

The soft form factor f^{NF}, obeying the large-energy symmetry relations [56], can be estimated in terms of a triangle diagram without a hard gluon exchange in the LCSR [38,57]. However, since the pion vertex has been replaced by the pion distribution amplitudes under twist expansion, what is calculated in the LCSR is not the full soft contribution. The term f^F has been expressed as a convolution of the hard-scattering kernel T' with the light-cone distribution amplitudes of the B meson and of the pion in the momentum fractions, implying that it is calculable in collinear factorization.

The second option is that an end-point singularity indicates the breakdown of the collinear factorization. Hence, the k_T factorization is the more appropriate framework, in which the parton transverse momenta k_T are retained in the hard kernel, and f^{EP} does not develop an end-point singularity. Both f^{EP} and f^F are then calculable, and expressed, in the PQCD approach, as

$$F^{B\pi} = f^{EP} + f^F = \phi_B \otimes T \otimes \phi_\pi, \qquad (33)$$

where the symbol $\otimes$ represents the convolution not only in the momentum fractions, but in the transverse separations. The hard kernel T' in Eq. (32) is derived from the complete hard kernel T by dropping the terms which led to the endpoint singularity in the collinear factorization. Certainly, the subtraction of these terms depends on a regularization scheme [55]. The strong Sudakov suppression in the soft parton region implies that the genuine soft contribution f^S is not important [8,24]. Equation (33) is then claimed to be a consequence of the hard-dominance picture, because a big portion of $F^{B\pi}$ is calculable. The agreement between the sum-rule and PQCD predictions for many B meson transition form factors justifies that f^S is indeed negligible. Since f^{EP} remains in Eq. (33), the form factor symmetry relations at large recoil are still respected in the PQCD framework [24], which are then modified by the subleading term f^F.

Therefore, the soft-dominance (hard-dominance) picture postulated in LCSR (PQCD) makes sense in the collinear (k_T) factorization [48]. The two pictures arise from the dif-

ferent theoretical frameworks, and there is no conflict at all. In other words, the soft contribution refers to f^{NF} in SCET, LCSR, and QCDF, which is large, but to f^S in PQCD, which is small. The LCSR can be regarded as a method to evaluate f^{EP} or f^{NF} in the collinear factorization (at least the light-cone distribution amplitudes have been employed on the pion side), while the k_T factorization is adopted in PQCD for the evaluation of f^{EP}. We emphasize that there is no preference between the two options for semileptonic B meson decays, both of which give similar results as stated above. However, in their extension to two-body nonleptonic B meson decays, predictions could be very different. For example, the main source of strong phases in the $B \to \pi\pi$ decays is the correction to the weak vertex in QCDF, but the annihilation diagram in PQCD. This is the reason QCDF (PQCD) predicts a smaller and positive (larger and negative) CP asymmetry $C_{\pi\pi}$ [14,58]. It is then possible to discriminate experimentally which theoretical framework works better.

Next we compare our formalism for two-body charmed nonleptonic B meson decays based on the k_T factorization with SCET and QCDF based on the collinear factorization. Currently, the LCSR has not yet been applied to the nonfactorizable contribution discussed here, but only to that from three-parton distribution amplitudes [59], since the former, involving two loops, is more complicated to analyze. Similarly, the neglect of k_T results in end-point singularities in the factorizable contributions ξ_{ext} and ξ_{int}, which need to be parametrized in terms of the $B \to D$ and $B \to \pi$ transition form factors, respectively. It also causes an end-point singularity in the color-suppressed nonfactorizable amplitude $\mathcal{M}_{int}$, if the c quark is treated as being massive. This is why the color-suppressed modes, i.e., the magnitude and the phase of a_2, cannot be predicted in QCDF, and the proof of QCDF in the SCET formalism [60] considered only the color-allowed mode $\bar{B}^0 \to D^+ \pi^-$. The color-allowed nonfactorizable amplitude $\mathcal{M}_{ext}$ is calculable in QCDF, because the end-point singularities cancel between the pair of diagrams Figs. 4(c) and 4(d). We mention a recent work on SCET [61], in which the color-suppressed nonfactorizable amplitude has been parametrized as an expression similar to Eq. (31).

If the c quark is treated as being massless, the end-point singularities in the pair of color-suppressed nonfactorizable diagrams, Figs. 5(c) and 5(d), will cancel each other as in the charmless case [33,58]. This can be understood by examining the behavior of the integrand of $\mathcal{M}_{int}$ in Eq. (A12) in the dominant region with small x_3, noticing that the D meson distribution amplitude $\phi_D(x_2)$ would be symmetric under the exchange of x_2 and $1-x_2$ in the $m_c \to 0$ limit. However, the nonfactorizable contribution will become negligible in this limit, such that the amplitude $\mathcal{M}_{int}$, although calculable in QCDF, is not large enough to explain the $B \to D\pi$ data. It is then obvious that the PQCD approach has made a great contribution here: the nonfactorizable corrections to the naive factorizations of both the color-allowed and color-suppressed modes can be predicted, and the latter is found to be very important.

VI. CONCLUSION

In this paper we have analyzed the two-body charmed nonleptonic decays $B \to D^{(*)}M$ with $M = \pi$, ρ, and ω in the PQCD approach. This framework is based on the k_T factorization theorem, which is free of end-point singularities and gauge invariant. The k_T factorization theorem is more appropriate, when the end-point region of a momentum fraction is important, and collinear factorization theorem breaks down. By including the transverse degrees of freedom of partons in the evaluation of a hard kernel, and the Sudakov factors from k_T and threshold resummations, the virtual particles remain sufficiently off shell, and the end-point singularities do not exist. We have explained that there is no conflict between LCSR with the soft-dominance picture and PQCD with the hard-dominance picture, since the soft contributions refer to different quantities in the two theoretical frameworks.

The derivation of the factorization formulas for the $B \to D^{(*)}M$ decay amplitudes follow the power counting rules constructed in our previous work on the $B \to D^{(*)}$ transition form factors. Under the hierarchy $m_B \gg m_{D^{(*)}} \gg \bar{\Lambda}$, the B and $D^{(*)}$ meson wave functions exhibit a peak at the momentum fractions around $\bar{\Lambda}/m_B$ and $\bar{\Lambda}/m_{D^{(*)}}$, respectively. Up to leading power in $m_{D^{(*)}}/m_B$ and in $\bar{\Lambda}/m_{D^{(*)}}$, only a single B meson wave function and a single $D^{(*)}$ meson wave function are involved. The factorization formulas then become simpler than those for charmless decays. Moreover, the factorization formulas for all the $B \to D^{(*)}M$ modes are identical, except for the appropriate substitution of the masses, the decay constants, and the meson distribution amplitudes. We emphasize that there is no arbitrary parameter in our analysis (there are in QCDF), although all the universal inputs are not yet known precisely. The meson wave functions have been determined either from the semileptonic data or from the LCSR.

Being free from the end-point singularities, all topologies of decay amplitudes are calculable in PQCD, including the color-suppressed nonfactorizable one. This amplitude cannot be computed in QCDF based on the collinear factorization theorem due to the existence of the end-point singularities for a massive c quark. We have observed in PQCD that this amplitude, not suppressed by the Wilson coefficient (proportional to C_2/N_c), is comparable to the dominant color-allowed factorizable amplitude. It generates a large strong phase from the nonpinched singularity of the hard kernel, which is crucial for explaining the observed $B \to D^{(*)}M$ branching ratios. The other topologies are less important: the color-allowed nonfactorizable contribution is negligible because of the pair cancellation and the small Wilson coefficient C_1/N_c. The color-suppressed factorizable amplitude with the small Wilson coefficient $a_2 = C_1 + C_2/N_c$ is also negligible. The annihilation amplitudes are small, since they come from the tree operators.

All our predictions are consistent with the existing measurements. For those without data, such as the $B \to D^{*0}\rho^0, D^{*0}\omega$ modes, our predictions can be confronted with future measurement. As stated before, we predicted the large strong phases from the scalar-penguin annihilation amplitudes that are required by the large CP asymmetries observed in two-body charmless decays. The success in predicting the strong phases from the color-suppressed nonfactorizable amplitudes for the two-body charmed decays

further supports the k_T factorization theorem. The conclusion drawn in this work is that the short-distance strong phase is already sufficient to account for the $B \rightarrow D^{(*)}M$ data. Certainly, there is still room for long-distance strong phases from final-state interaction. For the application of the PQCD approach to other charmed decays, such as $B \rightarrow D_s^{(*)}K$ and $B \rightarrow D^{(*)}f_0$, refer to [62] and [63], respectively.

ACKNOWLEDGMENTS

APPENDIX: FACTORIZATION FORMULAS FOR $B \rightarrow D\pi$

In this appendix we present the factorization formulas for the $B \rightarrow D\pi$ decay amplitudes. We choose the B meson, D meson, and pion momenta in the light-cone coordinate as

$$P_1 = \frac{m_B}{\sqrt{2}}(1,1,\mathbf{0}_T), \quad P_2 = \frac{m_B}{\sqrt{2}}(1,r^2,\mathbf{0}_T),$$

$$P_3 = \frac{m_B}{\sqrt{2}}(0,1-r^2,\mathbf{0}_T), \tag{A1}$$

respectively, with $r = m_D/m_B$ being defined before. The fractional momenta of the light valence quarks in the B meson, D meson, and pion are

$$k_1 = \begin{cases} x_1\dfrac{m_B}{\sqrt{2}}(1,0,\mathbf{0}_T) + \mathbf{k}_{1T} & \text{for } \xi_{\text{int}}, M_{\text{int}}, \\[3mm] x_1\dfrac{m_B}{\sqrt{2}}(0,1,\mathbf{0}_T) + \mathbf{k}_{1T} & \text{for others,} \end{cases}$$

$$k_2 = x_2\frac{m_B}{\sqrt{2}}(1,0,\mathbf{0}_T) + \mathbf{k}_{2T},$$

$$k_3 = x_3\frac{m_B}{\sqrt{2}}(0,1-r^2,\mathbf{0}_T) + \mathbf{k}_{3T}, \tag{A2}$$

respectively. Which longitudinal component of k_1, k_1^+ or k_1^-, is relevant depends on the final-state meson to which the hard gluon attaches. That is, it is selcted by the inner product $k_1 \cdot k_3$ or $k_1 \cdot k_2$.

The factorizable amplitudes ξ_{ext}, ξ_{int}, and ξ_{exc} are written as

$$\xi_{\text{ext}} = 16\pi C_F \sqrt{r} m_B^2 \int_0^1 dx_1 dx_2 \int_0^{1/\Lambda} b_1 db_1 b_2 db_2$$
$$\times \phi_B(x_1,b_1)\phi_D(x_2)[E_e(t_e^{(1)})h(x_1,x_2,b_1,b_2)S_t(x_2)$$
$$+ rE_e(t_e^{(2)})h(x_2,x_1,b_2,b_1)S_t(x_1)], \tag{A3}$$

$$\xi_{\text{int}} = 16\pi C_F \sqrt{r} m_B^2 \int_0^1 dx_1 dx_3 \int_0^{1/\Lambda} b_1 db_1 b_3 db_3 \phi_B(x_1,b_1)$$
$$\times (\{(1+x_3)\phi_\pi(x_3) + r_0(1-2x_3)[\phi_\pi^p(x_3) + \phi_\pi^t(x_3)]\}$$
$$\times E_i(t_i^{(1)})h[x_1,x_3(1-r^2),b_1,b_3]S_t(x_3)$$
$$+ 2r_0\phi_\pi^p(x_3)E_i(t_i^{(2)})h[x_3,x_1(1-r^2),b_3,b_1]S_t(x_1)), \tag{A4}$$

$$\xi_{\text{exc}} = 16\pi C_F \sqrt{r} m_B^2 \int_0^1 dx_2 dx_3 \int_0^{1/\Lambda} b_2 db_2 b_3 db_3 \phi_D(x_2)$$
$$\times \{-x_3\phi_\pi(x_3)E_a(t_a^{(1)})h_a[x_2,x_3(1-r^2),b_2,b_3]S_t(x_3)$$
$$+ x_2\phi_\pi(x_3)E_a(t_a^{(1)})h_a[x_3,x_2(1-r^2),b_3,b_2]S_t(x_2)\}, \tag{A5}$$

with the mass ratio $r_0 \equiv m_0/m_B$, the evolution factors,

$$E_e(t) = \alpha_s(t)a_1(t)\exp[-S_B(t)-S_D(t)],$$

$$E_i(t) = \alpha_s(t)a_2(t)\exp[-S_B(t)-S_\pi(t)],$$

$$E_a(t) = \alpha_s(t)a_2(t)\exp[-S_D(t)-S_\pi(t)], \tag{A6}$$

and the Wilson coefficients,

$$a_1 = C_2 + \frac{C_1}{N_c}, \quad a_2 = C_1 + \frac{C_2}{N_c}. \tag{A7}$$

Note that $C_1 = 0$ and $C_2 = 1$ at the tree level in our convention. The explicit expressions of the Sudakov factors $\exp[-S_B(t)]$, $\exp[-S_D(t)]$, and $\exp[-S_\pi(t)]$ from k_T resummation are taken from [20,24].

The functions h, obtained from Figs. 4(a) and 4(b), Figs. 5(a) and 5(b), and Figs. 6(a) and 6(b), are given by

$$h(x_1,x_2,b_1,b_2)$$
$$= K_0(\sqrt{x_1 x_2}m_B b_1)$$
$$\times [\theta(b_1-b_2)K_0(\sqrt{x_2}m_B b_1)I_0(\sqrt{x_2}m_B b_2)$$
$$+ \theta(b_2-b_1)K_0(\sqrt{x_2}m_B b_2)I_0(\sqrt{x_2}m_B b_1)], \tag{A8}$$

$$h_a(x_2,x_3,b_2,b_3)$$

$$=\left(i\frac{\pi}{2}\right)^2 H_0^{(1)}(\sqrt{x_2x_3}m_Bb_2)$$

$$\times[\theta(b_2-b_3)H_0^{(1)}(\sqrt{x_3}m_Bb_2)J_0(\sqrt{x_3}m_Bb_3)$$

$$+\theta(b_3-b_2)H_0^{(1)}(\sqrt{x_3}m_Bb_3)J_0(\sqrt{x_3}m_Bb_2)].$$

$$(A9)$$

The hard scales t are chosen as

$$t_e^{(1)}=\max(\sqrt{x_2}m_B,1/b_1,1/b_2),$$

$$t_e^{(2)}=\max(\sqrt{x_1}m_B,1/b_1,1/b_2),$$

$$t_i^{(1)}=\max(\sqrt{x_3(1-r^2)}m_B,1/b_1,1/b_3),$$

$$t_i^{(2)}=\max(\sqrt{x_1(1-r^2)}m_B,1/b_1,1/b_3),$$

$$t_a^{(1)}=\max(\sqrt{x_3(1-r^2)}m_B,1/b_2,1/b_3),$$

$$t_a^{(2)}=\max(\sqrt{x_2(1-r^2)}m_B,1/b_2,1/b_3).\quad(A10)$$

For the nonfactorizable amplitudes, the factorization formulas involve the kinematic variables of all the three mesons. Their expressions are

$$\mathcal{M}_{\text{ext}}=32\pi\sqrt{2N}C_F\sqrt{r}m_B^2\int_0^1[dx]$$

$$\times\int_0^{1/\Lambda}b_1db_1b_3db_3\phi_B(x_1,b_1)\phi_D(x_2)\phi_\pi(x_3)$$

$$\times[x_3E_b(t_b^{(1)})h_b^{(1)}(x_i,b_i)$$

$$-(1-x_3+x_2)E_b(t_b^{(1)})h_b^{(2)}(x_i,b_i)],\quad(A11)$$

$$\mathcal{M}_{\text{int}}=32\pi\sqrt{2N}C_F\sqrt{r}m_B^2\int_0^1[dx]$$

$$\times\int_0^{1/\Lambda}b_1db_1b_2db_2\phi_B(x_1,b_1)\phi_D(x_2)$$

$$\times[(-x_2-x_3)\phi_\pi(x_3)E_d(t_d^{(1)})h_d^{(1)}(x_i,b_i)$$

$$+(1-x_2)\phi_\pi(x_3)E_d(t_d^{(2)})h_d^{(2)}(x_i,b_i)],\quad(A12)$$

$$\mathcal{M}_{\text{exc}}=32\pi\sqrt{2N}C_F\sqrt{r}m_B^2\int_0^1[dx]$$

$$\times\int_0^{1/\Lambda}b_1db_1b_2db_2\phi_B(x_1,b_1)\phi_D(x_2)$$

$$\times[x_3\phi_\pi(x_3)E_f(t_f^{(1)})h_f^{(1)}(x_i,b_i)$$

$$-x_2\phi_\pi(x_3)E_f(t_f^{(2)})h_f^{(2)}(x_i,b_i)],\quad(A13)$$

from Figs. 4(c) and 4(d), Figs. 5(c) and 5(d), and Figs. 6(c) and 6(d), respectively, with the definition $[dx]\equiv dx_1dx_2dx_3$. The evolution factors are given by

$$E_b(t)=\alpha_s(t)\frac{C_1(t)}{N}\exp[-S(t)|_{b_2=b_1}],$$

$$E_d(t)=\alpha_s(t)\frac{C_2(t)}{N}\exp[-S(t)|_{b_3=b_1}],$$

$$E_f(t)=\alpha_s(t)\frac{C_2(t)}{N}\exp[-S(t)|_{b_3=b_2}].\quad(A14)$$

with the Sudakov exponent $S=S_B+S_D+S_\pi$.

The functions $h^{(j)}$, $j=1$ and 2, appearing in Eqs. (A11)–(A13), are written as

$$h_b^{(j)}=[\theta(b_1-b_3)K_0(Bm_Bb_1)I_0(Bm_Bb_3)$$

$$+\theta(b_3-b_1)K_0(Bm_Bb_3)I_0(Bm_Bb_1)]$$

$$\times\begin{cases}K_0(B_jm_Bb_3),&\text{for }B_j^2\geqslant0\\[2mm]\dfrac{i\pi}{2}H_0^{(1)}(\sqrt{|B_j^2|}m_Bb_3),&\text{for }B_j^2\leqslant0\end{cases}\quad(A15)$$

$$h_d^{(j)}=[\theta(b_1-b_2)K_0(Dm_Bb_1)I_0(Dm_Bb_2)$$

$$+\theta(b_2-b_1)K_0(Dm_Bb_2)I_0(Dm_Bb_1)]$$

$$\times\begin{cases}K_0(D_jm_Bb_2),&\text{for }D_j^2\geqslant0\\[2mm]\dfrac{i\pi}{2}H_0^{(1)}(\sqrt{|D_j^2|}m_Bb_2),&\text{for }D_j^2\leqslant0\end{cases}\quad(A16)$$

$$h_f^{(j)}=i\frac{\pi}{2}[\theta(b_1-b_2)H_0^{(1)}(Fm_Bb_1)J_0(Fm_Bb_2)$$

$$+\theta(b_2-b_1)H_0^{(1)}(Fm_Bb_2)J_0(Fm_Bb_1)]$$

$$\times\begin{cases}K_0(F_jm_Bb_1),&\text{for }F_j^2\geqslant0\\[2mm]\dfrac{i\pi}{2}H_0^{(1)}(\sqrt{|F_j^2|}m_Bb_1),&\text{for }F_j^2\leqslant0\end{cases}\quad(A17)$$

with the variables

$$B^2=x_1x_2,$$

$$B_1^2=x_1x_2-x_2x_3(1-r^2),$$

$$B_2^2=x_1x_2-x_2(1-x_3)(1-r^2),$$

$$D^2=x_1x_3(1-r^2),$$

$$D_1^2=F_1^2=(x_1-x_2)x_3(1-r^2),$$

$$D_2^2=(x_1+x_2)r^2-(1-x_1-x_2)x_3(1-r^2),$$

$$F^2=x_2x_3(1-r^2),$$

$$F_2^2 = x_1 + x_2 + (1 - x_1 - x_2) x_3 (1 - r^2).$$

(A18)

There is an ambiguity in defining a light-cone B meson wave function for the nonfactorizable amplitude $\mathcal{M}_{\text{exc}}$, since both the components k_1^+ and k_1^- contribute through the inner products $k_1 \cdot k_2$ and $k_1 \cdot k_3$ in the denominators of the virtual particle propagators. However, a careful examination of the factorization formula shows that the dominant region is the one with $k_2 \sim O(\bar{\Lambda})$ and $k_3 \sim O(m_B)$ at leading twist. Hence, we drop the term $k_1 \cdot k_2$. The scales $t^{(j)}$ are chosen as

$$t_b^{(j)} = \max(B m_B, \sqrt{|B_j^2|} m_B, 1/b_1, 1/b_3),$$

$$t_d^{(j)} = \max(D m_B, \sqrt{|D_j^2|} m_B, 1/b_1, 1/b_2),$$

$$t_f^{(j)} = \max(F m_B, \sqrt{|F_j^2|} m_B, 1/b_1, 1/b_2).$$

(A19)

We explain that the factorization formulas presented above are indeed of leading power under the power counting rules in [20]. The factorizable amplitudes are as shown in [20,33]. For the nonfactorizable amplitudes, the terms proportional to x_3 and to $1 - x_3$ in $\mathcal{M}_{\text{ext}}$ roughly cancel each other. This cancellation can be understood by means of the corresponding expression in collinear factorization theorem: the first and second terms in $\mathcal{M}_{\text{ext}}$ are proportional to

$$-\frac{x_3}{x_1 x_2^2 x_3}, \quad \frac{1 - x_3 + x_2}{x_1 x_2^2 (1 - x_3)}.$$

(A20)

For simplicity, x_1 has been suppressed, when it appears in the sum together with x_2 or x_3. It is found that the first ratio cancels the $1 - x_3$ term in the second ratio. That is, the x_2 term is in fact leading and not negligible. For a similar reason, the $-x_2$ term in $\mathcal{M}_{\text{int}}$ cancels the $1 - x_2$ term. Hence, the $-x_3$ term is leading. If one drops $-x_2$ in $\mathcal{M}_{\text{int}}$, the above cancellation disappears, and a fake leading term will be introduced.

The pion and ρ meson distribution amplitudes have been derived in [36,37]:

$$\phi_\pi(x) = \frac{3 f_\pi}{\sqrt{2 N_c}} x(1 - x)[1 + 0.44 C_2^{3/2}(2x - 1)$$

$$+ 0.25 C_4^{3/2}(2x - 1)],$$

(A21)

$$\phi_\pi^p(x) = \frac{f_\pi}{2\sqrt{2 N_c}}[1 + 0.43 C_2^{1/2}(2x - 1) + 0.09 C_4^{1/2}(2x - 1)],$$

(A22)

$$\phi_\pi^t(x) = \frac{f_\pi}{2\sqrt{2 N_c}}(1 - 2x)[1 + 0.55(10x^2 - 10x + 1)],$$

(A23)

$$\phi_\rho(x) = \frac{3 f_\rho}{\sqrt{2 N_c}} x(1 - x)[1 + 0.18 C_2^{3/2}(2x - 1)],$$

(A24)

$$\phi_\rho^t(x) = \frac{f_\rho^T}{2\sqrt{2 N_c}}\{3(2x - 1)^2 + 0.3(2x - 1)^2[5(2x - 1)^2 - 3]$$

$$+ 0.21[3 - 30(2x - 1)^2 + 35(2x - 1)^4]\},$$

(A25)

$$\phi_\rho^s(x) = \frac{3 f_\rho^T}{2\sqrt{2 N_c}}(1 - 2x)[1 + 0.76(10x^2 - 10x + 1)],$$

(A26)

$$\phi_\rho^T(x) = \frac{3 f_\rho^T}{\sqrt{2 N_c}} x(1 - x)[1 + 0.2 C_2^{3/2}(2x - 1)],$$

(A27)

$$\phi_\rho^v(x) = \frac{f_\rho}{2\sqrt{2 N_c}}\left\{\frac{3}{4}[1 + (2x - 1)^2] + 0.24[3(2x - 1)^2 - 1]\right.$$

$$\left. + 0.12[3 - 30(2x - 1)^2 + 35(2x - 1)^4]\right\},$$

(A28)

$$\phi_\rho^a(x) = \frac{3 f_\rho}{4\sqrt{2 N_c}}(1 - 2x)[1 + 0.93(10x^2 - 10x + 1)],$$

(A29)

with the Gegenbauer polynomials,

$$C_2^{1/2}(t) = \frac{1}{2}(3t^2 - 1), \quad C_4^{1/2}(t) = \frac{1}{8}(35t^4 - 30t^2 + 3),$$

$$C_2^{3/2}(t) = \frac{3}{2}(5t^2 - 1), \quad C_4^{3/2}(t) = \frac{15}{8}(21t^4 - 14t^2 + 1).$$

(A30)

We shall assume that the ω meson wave functions are identical to the ρ meson ones in this work.

[1] M. Bauer, B. Stech, and M. Wirbel, Z. Phys. C **29**, 637 (1985); **34**, 103 (1987).

[2] H.Y. Cheng, Phys. Lett. B **335**, 428 (1994).

[3] H.Y. Cheng, Z. Phys. C **69**, 647 (1996).

[4] J. Soares, Phys. Rev. D **51**, 3518 (1995); A.N. Kamal and A.B. Santra, Z. Phys. C **72**, 91 (1996); A.N. Kamal, A.B. Santra, and R.C. Verma, Phys. Rev. D **53**, 2506 (1996).

[5] M. Beneke, G. Buchalla, M. Neubert, and C.T. Sachrajda, Phys. Rev. Lett. **83**, 1914 (1999); Nucl. Phys. **B591**, 313 (2000).

[6] G.P. Lepage and S.J. Brodsky, Phys. Lett. **87B**, 359 (1979); Phys. Rev. D **22**, 2157 (1980).

[7] J. Botts and G. Sterman, Nucl. Phys. **B225**, 62 (1989).

[8] H-n. Li and G. Sterman, Nucl. Phys. **B381**, 129 (1992).

[9] H-n. Li and H.L. Yu, Phys. Rev. Lett. **74**, 4388 (1995); Phys. Lett. B **353**, 301 (1995); Phys. Rev. D **53**, 2480 (1996).

[10] C.H. Chang and H-n. Li, Phys. Rev. D **55**, 5577 (1997).

[11] T.W. Yeh and H-n. Li, Phys. Rev. D **56**, 1615 (1997).

[12] H.Y. Cheng, H-n. Li, and K.C. Yang, Phys. Rev. D **60**, 094005 (1999).

[13] H-n. Li, Phys. Rev. D **64**, 014019 (2001); M. Nagashima and H-n. Li, hep-ph/0202127; Phys. Rev. D **67**, 034001 (2003).

[14] Y.Y. Keum, H-n. Li, and A.I. Sanda, Phys. Lett. B **504**, 6 (2001); Phys. Rev. D **63**, 054008 (2001); Y.Y. Keum and H-n. Li, *ibid.* **63**, 074006 (2001).

[15] C.D. Lü, K. Ukai, and M.Z. Yang, Phys. Rev. D **63**, 074009 (2001).

[16] Y.Y. Keum and A.I. Sanda, Phys. Rev. D **67**, 054009 (2003).

[17] Y.Y. Keum, hep-ph/0210127.

[18] Y.Y. Keum, hep-ph/0209208.

[19] M. Neubert and A.A. Petrov, Phys. Lett. B **519**, 50 (2001).

[20] T. Kurimoto, H-n. Li, and A.I. Sanda, Phys. Rev. D **67**, 054028 (2003).

[21] A.P. Szczepaniak, E.M. Henley, and S.J. Brodsky, Phys. Lett. B **243**, 287 (1990); G. Burdman and J.F. Donoghue, *ibid.* **270**, 55 (1991).

[22] J.C. Collins and D.E. Soper, Nucl. Phys. **B193**, 381 (1981).

[23] H-n. Li, Phys. Rev. D **66**, 094010 (2002).

[24] T. Kurimoto, H-n. Li, and A.I. Sanda, Phys. Rev. D **65**, 014007 (2002).

[25] H-n. Li and K. Ukai, Phys. Lett. B **555**, 197 (2003).

[26] M. Neubert, V. Rieckert, B. Stech, and Q.P. Xu, in *Heavy Flavours*, edited by A.J. Buras and M. Lindner (World Scientific, Singapore, 1992), p. 286; M. Neubert and B. Stech, in *Heavy Flavours II*, edited by A.J. Buras and M. Lindner (World Scientific, Singapore, 1998), p. 294, hep-ph/9705292.

[27] A. Deandrea, N. Di Bartolomeo, R. Gatto, and G. Nardulli, Phys. Lett. B **318**, 549 (1993).

[28] H.Y. Cheng and K.C. Yang, Phys. Rev. D **59**, 092004 (1999).

[29] Belle Collaboration, K. Abe *et al.*, Phys. Rev. Lett. **88**, 052002 (2002).

[30] CLEO Collaboration, T.E. Coan *et al.*, Phys. Rev. Lett. **88**, 062001 (2002); Phys. Rev. D **59**, 092004 (1999).

[31] H.Y. Cheng, Phys. Rev. D **65**, 094012 (2002).

[32] For a review, see G. Buchalla, A.J. Buras, and M.E. Lautenbacher, Rev. Mod. Phys. **68**, 1125 (1996).

[33] C.H. Chen, Y.Y. Keum, and H-n. Li, Phys. Rev. D **64**, 112002 (2001); **66**, 054013 (2002).

[34] C.Y. Wu, T.W. Yeh, and H-n. Li, Phys. Rev. D **53**, 4982 (1996); **55**, 237 (1997).

[35] A. Ali, G. Kramer, and C.D. Lü, Phys. Rev. D **58**, 094009 (1998); C.D. Lü, Nucl. Phys. B (Proc. Suppl.) **74**, 227 (1999); Y.H. Chen, H.Y. Cheng, B. Tseng, and K.C. Yang, Phys. Rev. D **60**, 094014 (1999).

[36] P. Ball, J. High Energy Phys. **01**, 010 (1999).

[37] P. Ball, V.M. Braun, Y. Koike, and K. Tanaka, Nucl. Phys. **B529**, 323 (1998).

[38] P. Ball and V.M. Braun, Phys. Rev. D **58**, 094016 (1998); P. Ball, J. High Energy Phys. **09**, 005 (1998); A. Khodjamirian *et al.*, Phys. Rev. D **62**, 114002 (2000).

[39] V.N. Baier and A.G. Grozin, hep-ph/9908365, and references therein.

[40] BaBar Collaboration, B. Aubert *et al.*, hep-ex/0207092.

[41] M. Gourdin, A.N. Kamal, Y.Y. Keum, and X.Y. Pham, Phys. Lett. B **333**, 507 (1994).

[42] Z.Z. Xing, hep-ph/0107257.

[43] C.K. Chua, W.S Hou, and K.C. Yang, Phys. Rev. D **65**, 096007 (2002).

[44] J.P. Lee, hep-ph/0109101.

[45] Particle Data Group, K. Hagawara *et al.*, Phys. Rev. D **66**, 010001 (2002).

[46] C.W. Chiang and J.L. Rosner, Phys. Rev. D **67**, 074013 (2003).

[47] A.I. Sanda, N. Sinha, R. Sinha, and K. Ukai, in *Proceedings of the 4th Workshop on B Physics and CP Violation (BCP4)*, edited by T. Ohshima and A.I. Sanda (World Scientific, Singapore, 2001), p. 339.

[48] H.-n. Li, Prog. Part. Nucl. Phys. **51**, 85 (2003).

[49] C.W. Bauer, S. Fleming, and M. Luke, Phys. Rev. D **63**, 014006 (2001).

[50] C.W. Bauer, S. Fleming, D. Pirjol, and I.W. Stewart, Phys. Rev. D **63**, 114020 (2001).

[51] V.L. Chernyak and I.R. Zhitnitsky, Nucl. Phys. **B345**, 137 (1990).

[52] A. Ali, V.M. Braun, and H. Simma, Z. Phys. C **63**, 437 (1994).

[53] H-n. Li, hep-ph/0304217.

[54] D. Pirjol and I.W. Stewart, Phys. Rev. D **67**, 094005 (2003); **69**, 019903 (2004).

[55] M. Beneke and T. Feldmann, Nucl. Phys. **B592**, 3 (2000).

[56] J. Charles *et al.*, Phys. Rev. D **60**, 014001 (1999); J. Chay and C. Kim, *ibid.* **65**, 114016 (2002); M. Beneke, A.P. Chapovsky, M. Diehl, and T. Feldmann, Nucl. Phys. **B643**, 431 (2002).

[57] P. Ball, hep-ph/0308249.

[58] H-n. Li, hep-ph/0110365.

[59] A. Khodjamirian, Nucl. Phys. **B605**, 558 (2001); B. Melic, Phys. Rev. D **68**, 034004 (2003).

[60] C.W. Bauer, D. Pirjol, and I.W. Stewart, Phys. Rev. Lett. **87**, 201806 (2001).

[61] S. Mantry, D. Pirjol, and I.W. Stewart, Phys. Rev. D **68**, 114009 (2003).

[62] C.D. Lu and K. Ukai, Eur. Phys. J. C **28**, 305 (2003); Y. Li and C.D. Lu, J. Phys. G **29**, 2115 (2003).

[63] C.H. Chen, Phys. Rev. D **67**, 094011 (2003).